

**ENGR527/727-001****FINAL PROJECT**

**Joby M. Anthony III <jmanthony1@liberty.edu>, Carson W. Farmer**

PhD Students

**ABSTRACT**

*As the consumption of sugary, carbonated drinks has increased in recent years, an overwhelming number of aluminum cans have entered waste disposal facilities. To reduce the spatial requirement of the individual cans, we propose a rotationally driven high-throughput can crushing device that operates either via human or machine power to easily deform cans to at least 20% of the original volume. By utilizing a varying thickness wheel, the rotation of the wheel functions as a cam to compress the can against the wall of the device to less than 20% of the volume. The shaft is constructed from AISI 316 while the crushing wheel is cast stainless steel. A finite element study was conducted to verify that the stresses experienced in the design did not surpass the yield stresses of the components. The proposed device solves the issue of crushing cans and allows for automatic reloading to allow for continuous operation.*

**Keywords:** *foo, bar*

**NOMENCLATURE**

$\tau$  = shear stress

$\theta$  = angular displacement

$a$  = height of the hexagonal cross-section

$b$  = base of rectangular cross-section

$h$  = height of rectangular cross-section

$F$  = force applied at the end of the handle

$M$  = resultant moment from the force applied to the handle

$T$  = torque applied to the shaft

$y$  = distance from neutral axis for bending stress

$G$  = shear modulus

$L$  = handle length

**1. INTRODUCTION**

As the consumption of soda continues to increase internationally, landfills are being overwhelmed by the number of empty cans produced. Current estimates by the EPA predict that 1.9 millions tons of aluminum are produced as beverage packaging [1] (PER YEAR??). To improve the ability to transport the cans to either a recycling facility or a landfill, a reduction of volume is necessary to decrease the required space and increase the ability to transport more cans in a single delivery. Can crushing mechanisms are typically either human-powered or complex electro-mechanical machines. The human aspect of the design encourages people to be engaged in the recycling process and be conscious of their choices. However, creating an electrically driven device automates process and provides capability for high throughput crushing.

In the design of the device, a survey of similar can crushing devices was performed to understand the required features for the desired device. Next, the design was formulated and components were selected from common part providers or were designed to be easily fabricated. To ensure the feasibility of the design and materials selection, an analytical analysis of two key points was conducted along with a Finite Element Analysis (FEA) of the entire system at the maximum crushing force of the can. Lastly, a comparison of the FEA results with the fatigue life of the components ensures that the device meets the requirements for an infinite life design.

## 2. DEVELOPMENT OF ENGINEERING SPECIFICATIONS

To develop the specifications for the design, several considerations were made to ensure that the design would be constructed effectively and within the limits of human strength. First, the average pulling force for a human was determined to be  $20 \text{ lb}_f$  which is consistent with NASA standards [2]. In an effort to reduce the environmental impact of the design, the additional constraint of purchasing as many parts as possible without requiring custom fabricated parts. In the final design, less than half of the parts required were custom designed. The remainder were able to be purchased from McMaster-Carr.

To determine the required crushing force for an aluminum beverage can, six uniaxial compression tests were conducted and the results are shown in Fig. 2-1. The average maximum crushing force was found to be approximately  $1.3 \text{ kN}$  to reduce the can to 20% of the original volume. For the dimensions of an aluminum beverage can, the can was considered to have an original height of  $157 \text{ mm}$  and to achieve 80% reduction in volume, the can would need to be deformed to a thickness of  $31.4 \text{ mm}$ . The dimensions of the can were determined via measurements taken from the beverage cans used in the compression tests. Furthermore, from the project instructions, the final design was required to have the ability to be either mechanically or electrically driven. Additionally, the requirement of having the crushing mechanism automatically reload was added to improve the total throughput of the cans to be crushed. The metric for the human force and crushing force are determined via mechanical analysis. For the material selection, the commercially listed for the components will be used in the design.

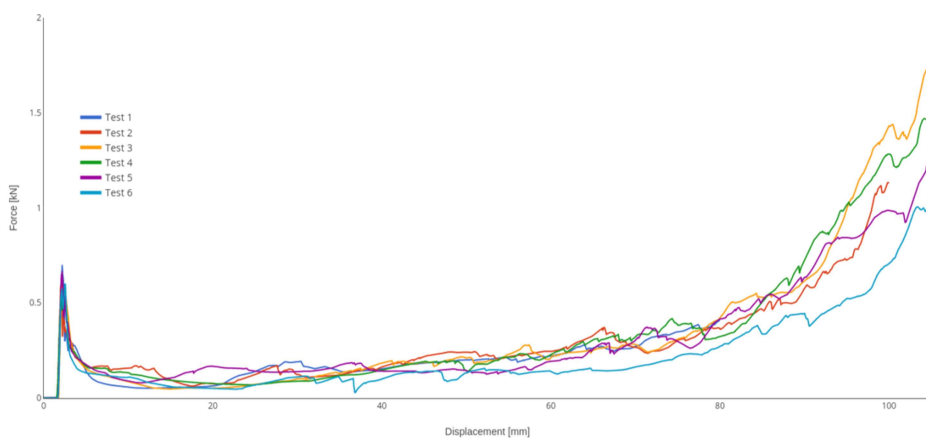


**FIGURE 2-1.** RESULTS FROM CRUSHING SIX DIFFERENT ALUMINUM SODA CANS WITH THE REGIONS OF BUCKLING AND MAXIMUM FORCE DENOTED.

## 3. SYNTHESIS OF THE DESIGN

In creating the final design of the system, several commercially and custom fabricated can crushing solutions were considered. While the common lever-based design (Fig. 3-2) allows for a can to be easily crushed, the challenge arises in creating an automated and high-throughput can crushing device. The common industrial devices serve to shred rather than compress the aluminum cans for use in recycling facilities. By investigating Do-It-Yourself (DIY) designs, a common method for automating the process is to create a crank-slider mechanism to compress the can. However, the number of moving parts in the design creates a higher likelihood of component failure if the device is operated for long periods of time.

The design of the proposed device functions on the use of a "cam" with varying thickness to compress the aluminum can against the wall of the device. The thickness of the cam varies angularly allowing for a gradual crushing of the can. Once the can has been reduced to 20% of the original volume, the can exits the device via a slot in the bottom of the housing. As the wheel completes a revolution, the opening for a can reaches the can entry location and allows the can to drop into the crushing area. The cam is suggested to be made from cast stainless steel.

The shaft of the cam is hexagonal and purchased from McMaster-Carr and is made from AISI 316 [3]. In the current iteration, a handle purchased from McMaster-Carr [4] is attached to the shaft and a human is expected to provide the required rotational input to the device. However, a coupler could be used to attach the shaft to a motor to improve the rate of compression for the cans. The device is shown in Fig. 3-1.

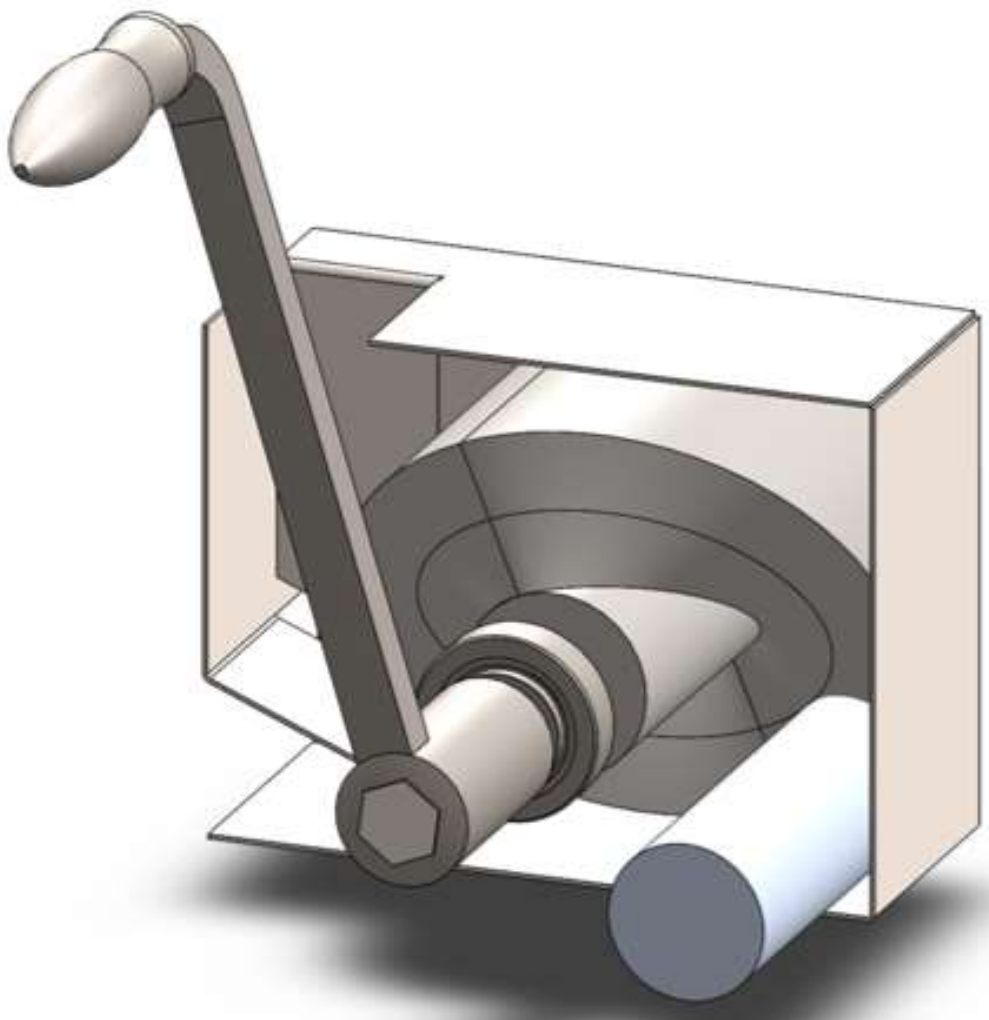


**FIGURE 3-1.** DESIGN OF THE CAN CRUSHING DEVICE WITH A PORTION OF THE HOUSING CUT AWAY TO VIEW INTERNAL CRUSHING CHAMBER.



**FIGURE 3-2.** EXAMPLE OF A COMMON DESIGN FOR MANUAL CAN CRUSHING DEVICES.

## 4. DESIGN ANALYSIS AND OPTIMIZATION

For analyzing the design of the can crushing mechanism, the analysis was broken down into two type: analytical and FEA. The analytical work focused on two points of interested: a point on the handle, and a point on the cross-section of the shaft. Due to the complex geometry of the cam, a FEA was carried out on the part assuming the maximum possible load applied by a human.

### 4.1. Analytical Methods

#### 4.1.1. SHAFT CROSS-SECTION

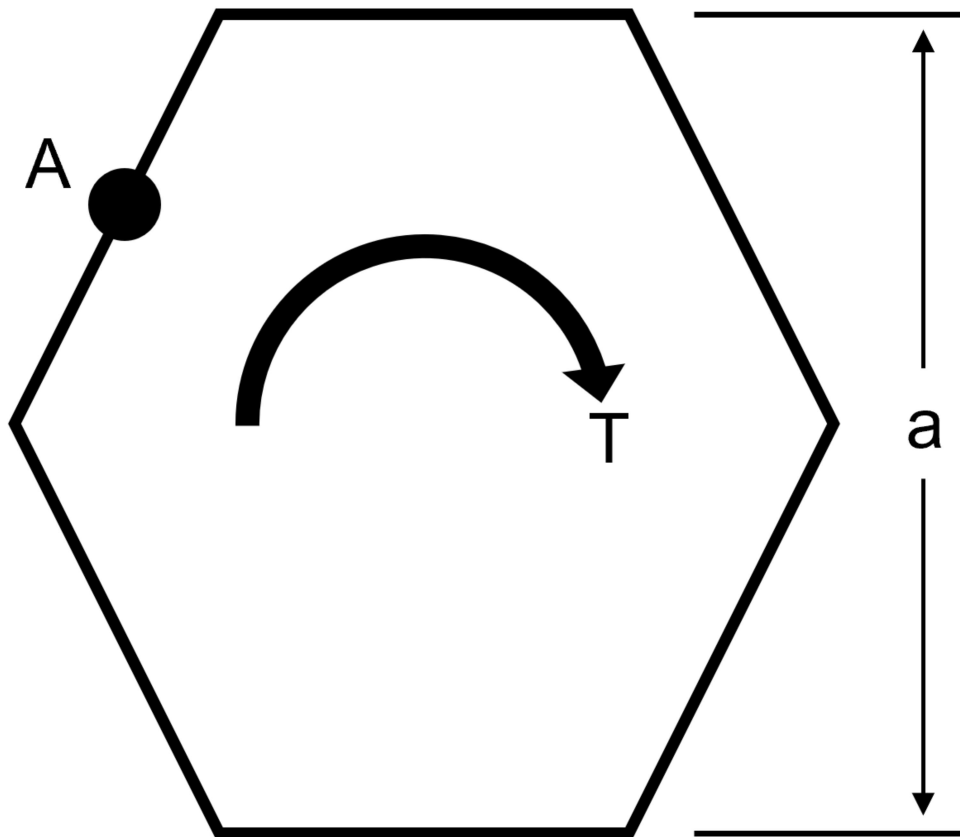


**FIGURE 4-1.** DIAGRAM FOR THE HEXAGONAL SHAFT CROSS-SECTION WITH THE APPLIED TORQUE AND KEY DIMENSIONS HIGHLIGHTED.

From Table 6.2 in [5], the equations for the maximum shear stress,  $\tau_A$ , and angular deflection,  $\theta$ , for a hexagonal cross-section. The free body diagram for the torque applied to the shaft is shown in Fig. 4-1. To calculate the shear stress and deflection, the equations for shear stress and deflection from the textbook [5]:

$$\tau_A = \frac{5.7T}{a^3} \quad \theta = \frac{8.8T}{a^4G} L \quad (1)$$

where  $T$  is the applied torque,  $a$  is the height of the hexagon, and  $G$  is the modulus of rigidity. From the geometry of the shaft,  $a = 1 \text{ in}$ . For AISI 316, the shear modulus,  $G = 78 \text{ GPa}$ . For an applied torque of  $220 \text{ lbf} \cdot \text{in}$ , the maximum shear stress is predicted to be  $8.646 \text{ MPa}$  which closely matches the FEA results. Furthermore, the maximum predicted deflection is  $2.05 \text{ milliradians}$ . The deflection of the rod predicted via this equation is not comparable to the FEA results since the effects of the cam prevent some of the deflection that would be experienced by the shaft.

#### 4.1.2. HANDLE

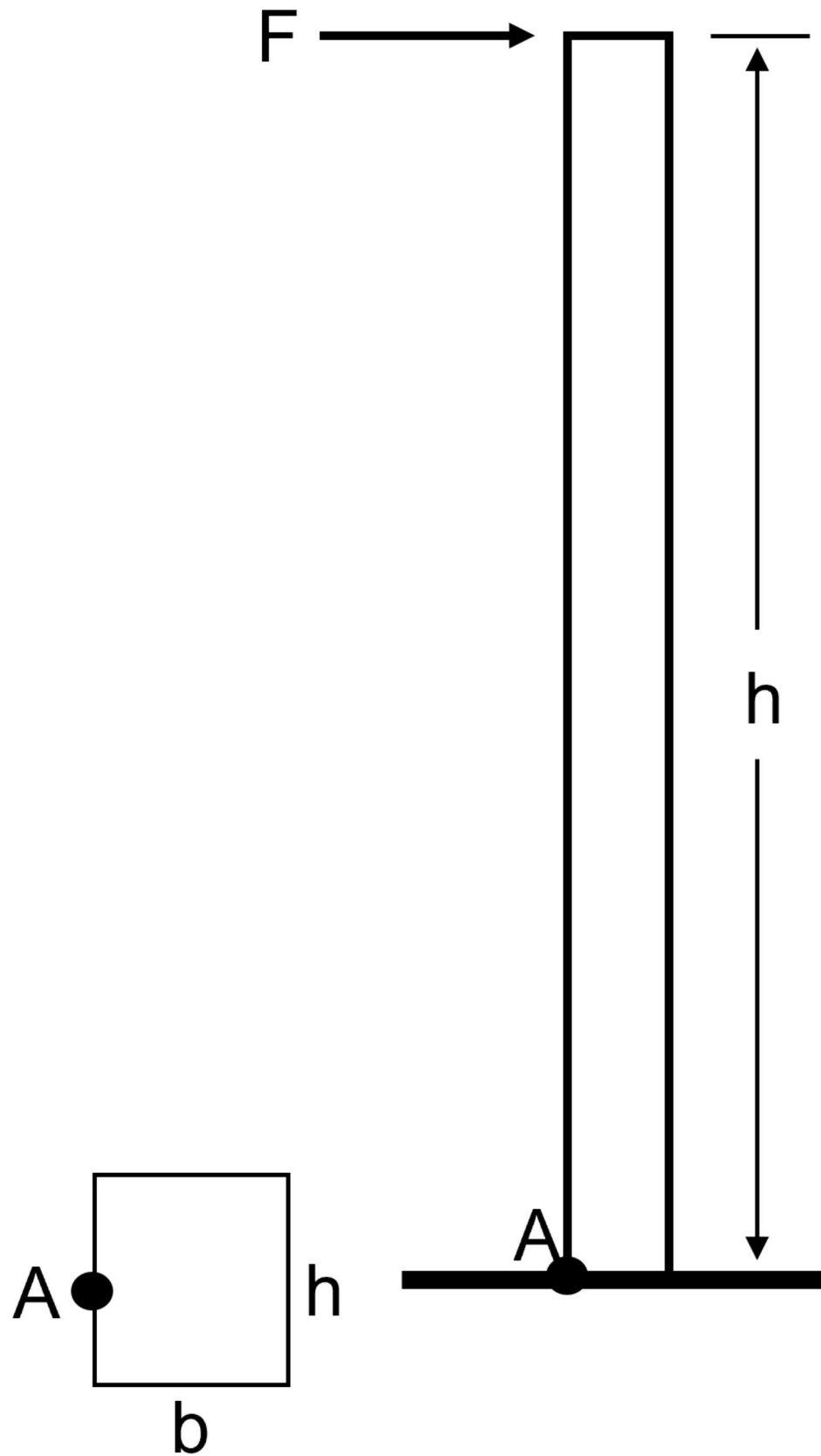


**FIGURE 4-2.** FBD FOR THE HANDLE TO DETERMINE THE MAXIMUM BENDING STRESS AT THE CONNECTION.

The handle of the mechanism is subject to a moment produced by the force applied to the handle (see Fig. 4-2). Since the cross-section of the bar is rectangular, the standard equation for bending is applied. At the end of the handle, a force of  $20 \text{ lb}_f$ , which is the human strength found from NASA [2], is applied. The handle has a length,  $L = 11 \text{ in}$  with a cross-sectional area of  $\text{in}^2$ .

0.75 inches  $\times$  0.6 in. Using the equation for bending stress at point A on the cross-section:

$$\sigma_A = \frac{M y}{I} \quad (2)$$

where  $M = 20 \text{ lb}_f * 10.125 \text{ in} = 202.5 \text{ lb}_f \cdot \text{in}$ ,  $y = 0.375 \text{ in}$ , and  $I = \frac{1}{12}(0.6 \text{ in})(0.75 \text{ in})^3$ . This gives a maximum normal stress of 24.8 MPa. Once again, this closely matches the results determined in the FEA analysis near the point of interest.

#### 4.1.3. CONCLUSIONS

Within the brief analytical work conducted, both the shear stress in the shaft and the maximum normal stress are both well below the limits of the material. For the cam, an FEA approach is employed due to the complex geometry of the contact surface with the can. The checks provided by the analytical work confirm that the FEA results are close to the predicted values.

### 4.2. Finite Element Analysis (FEA)

Referring to [Sec. 4.1](#), recall that the maximum shear stress calculated for the shaft was 8.646 MPa, and the maximum stress due to bending in the handle was calculated to be 24.8 MPa. Mechanical loads of 202.5 lb<sub>f</sub> · in and 1.3 kN were applied to the handle and the crushing face of the cam, respectively. The input torque causes the shaft to rotate which, in turn, forces the can to be crushed by the reduction of available space from the cam. If the cam withstands the average reacting force from the can (1.3 kN), then the cam should also withstand every prerequisite reaction force (as seen in the force-displacement curve [Fig. 2-1](#)). Finite Element Analyses were carried out in **SolidWorks 2016-17** to verify these analytical calculations for the maximum stresses seen in the shaft and handle. A mesh refinement study was also performed to validate the FEA results.

#### 4.2.1. MESH REFINEMENT

To determine the appropriate mesh element size and the sufficient number of elements needed for calculations, the mesh element size is gradually decreased such that the number of mesh elements increases. The more elements there exist in a study, the more precise the solution will be. However, the solution will take much longer to solve which may also become more inaccurate due to truncation errors.

To demonstrate this concept clearly, [Fig. 4-3](#) plots the percent difference of the maximum shear stress seen in the shaft between some mesh and the next finer mesh. By increasing the number of mesh elements, the percent difference decreases from  $\sim 15\%$  at 14,479 elements down to  $\sim 1\%$  at 56,842 elements. However, there is a considerable spike back up  $\sim 20\%$  at 392,144 elements. For the selected mesh element size of 0.2 in and 56,842 number of elements, this mesh may be seen in [Fig. 4-4](#).

Mesh Refinement Study Based on Maximum Shear Stress in Hexagonal Shaft

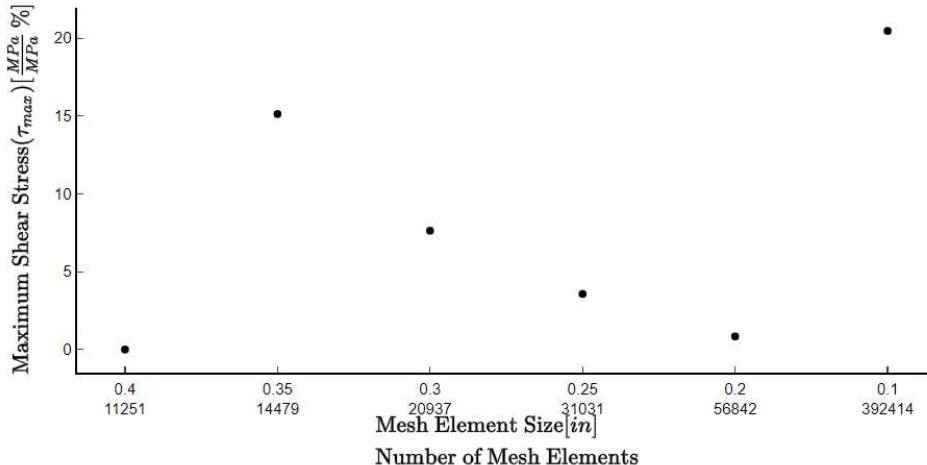
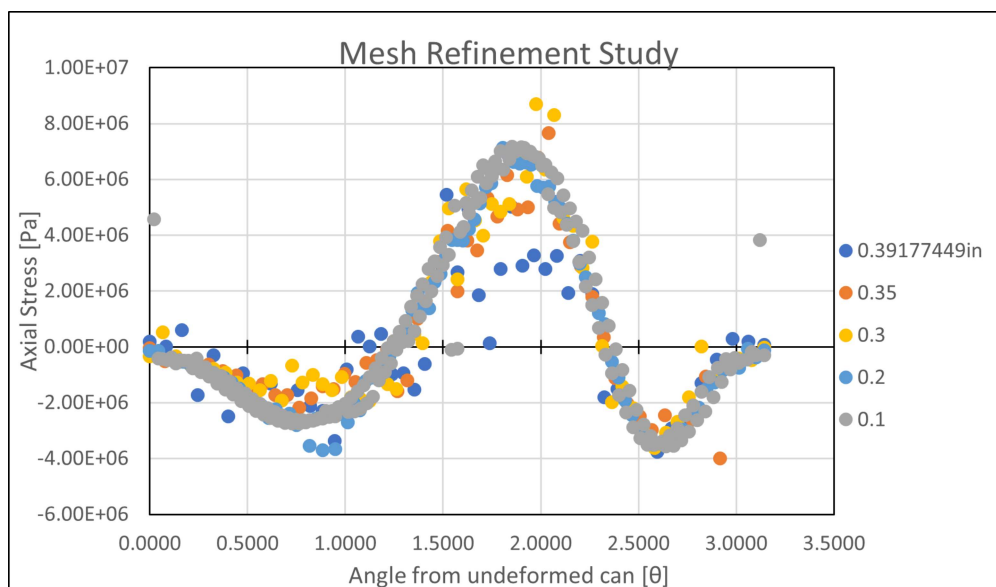


FIGURE 4-3. INCREASING THE NUMBER OF MESH ELEMENTS REVEALED THAT THE MESH ELEMENT SIZE OF 0.2 in WAS SUFFICIENT AND WAS THEREFORE USED FOR SIMULATION STUDIES REPORTED FOR THE REMAINDER OF THIS WORK.



**FIGURE 4-4. BAR**

To further demonstrate the importance of performing a mesh refinement study, examine Fig. 4-5. Measured at the contacting line between the crushing face of the cam and the top of the can (best visualized in Fig. 4-6), the stress normal to the axis of the shaft was observed to vary radially. The  $x$ -axis of this plot is in the domain  $[0, \pi]$  because the cam requires only  $180^\circ$  rotation to crush the can. The stresses are in the axial direction of the shaft and have a positive sense toward where the handle connects to the shaft.



**FIGURE 4-5. RADIAL DISTRIBUTION OF NORMAL STRESS IN THE SHAFT AXIAL DIRECTION AT THE CONTACTING LINE BETWEEN THE CRUSHING FACE OF THE CAM AND THE TOP OF THE CAN FOR VARIOUS MESH ELEMENT SIZES.**

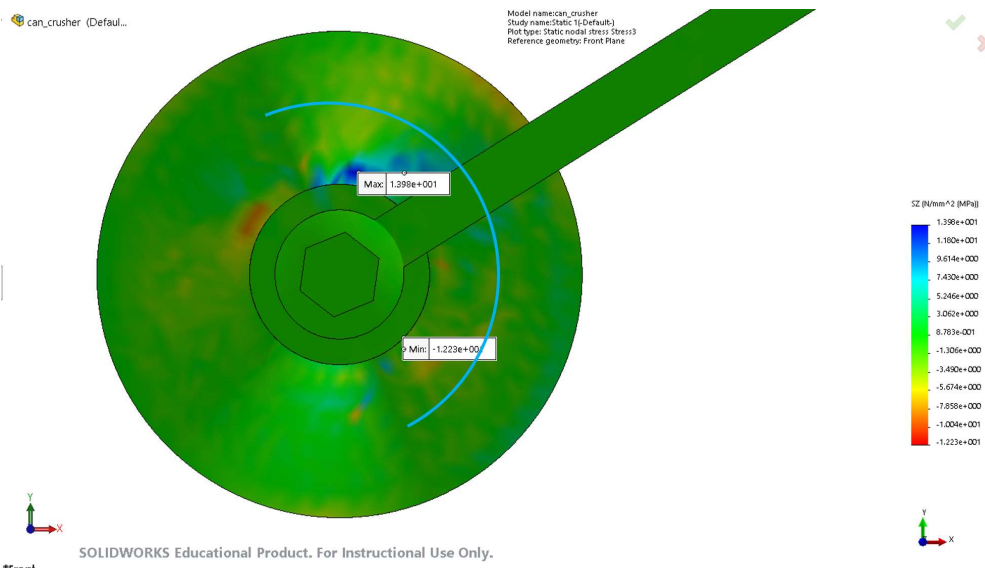


**FIGURE 4-6.** THE MAXIMUM NORMAL STRESS IN THE SHAFT AXIAL DIRECTION OF  $\sim 7 \text{ MPa}$  (FIG. 4-5) OCCURS AT THE RIGHTMOST EXTREME OF THE CONTACT LINE AS SHOWN.

#### 4.2.2. KEY COMPONENTS

To corroborate those values calculated from Sec. 4.1, the effects from the applied input torque and average reaction force were examined in the shaft, handle, and contacting face of the cam. A single simulation was performed on the connected handle, shaft, inner ring of the bearings, and the cam. The chamber housing and the other parts of the bearings were excluded from this particular simulation because those components are not the focus of this design.

##### SHAFT

The shear strength of AISI 316 stainless steel is known to be in the range [74.5, 597.0] MPa [6]. The maximum shear stress in the shaft of 9.171 MPa yields a factor of safety in the range of [8.12, 65.10]. Therefore, selection of this hexagonal shaft was sufficient for this design and the results from the FEA study differed from the analytical calculation (8.646 MPa) by 5.89%.

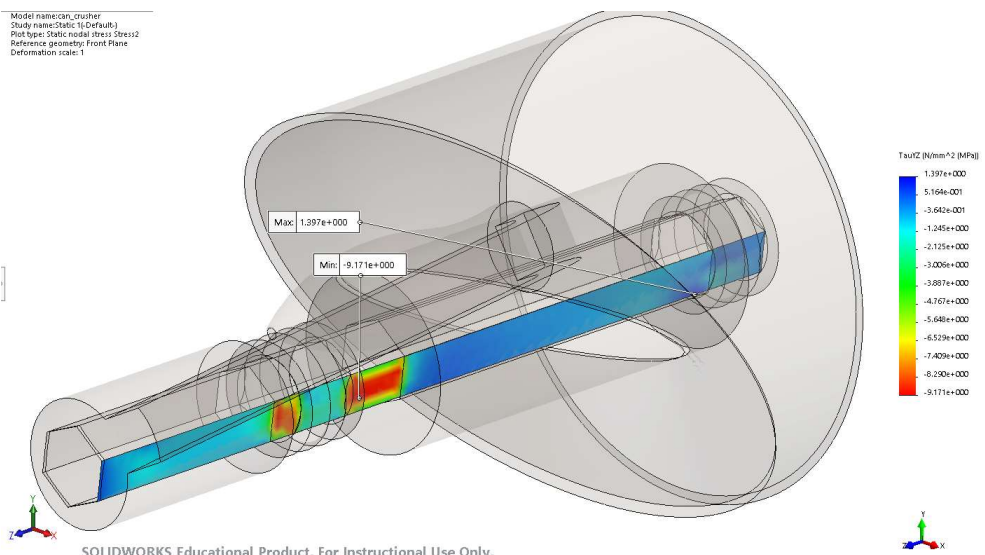


**FIGURE 4-7.** A MAXIMUM SHEAR STRESS OF 9.171 MPa MAY BE SEEN AT THE SHAFT SURFACE BETWEEN THE CAM AND BEARING.

##### HANDLE

**SolidWorks** lists the yield strength of 1023 carbon steel to be 282.69 MPa. The maximum bending stress in the handle of 34 MPa yields a factor of safety of 8.31. Therefore, selection of this 11 in handle to fit the hexagonal shaft was sufficient for this design and the results from the FEA study differed from the analytical calculation (24.8 MPa) by 31.29%. This large disparity is

likely due to how the average reaction force from the can acts on the crushing face of the cam because of the complex surface geometry which cannot be so simplified as a simple torque for hand calculations.

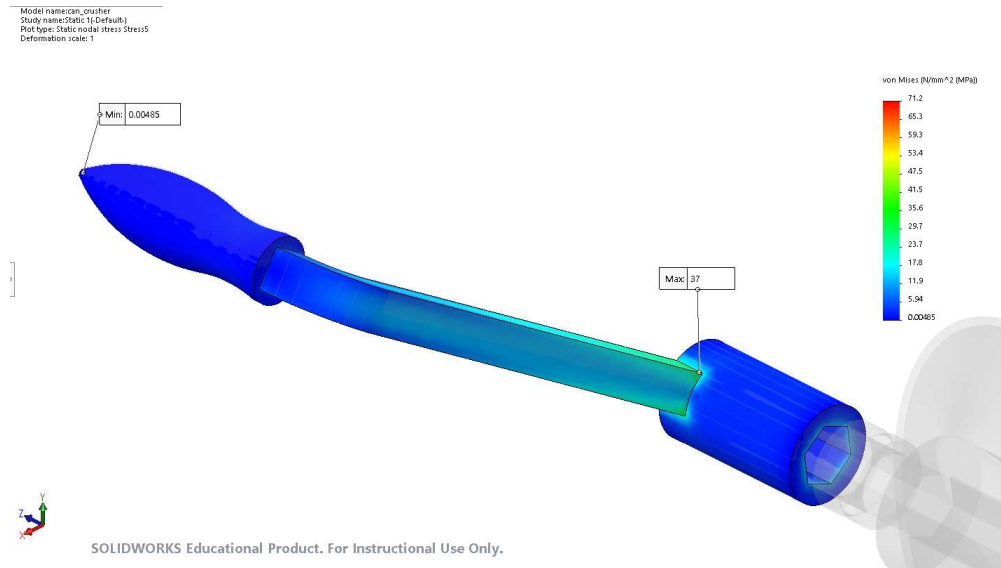


**FIGURE 4-8.** A MAXIMUM BENDING STRESS OF 34 MPa OCCURS AT THE POINT IN THE ARM OF THE HANDLE CLOSE TO THE SHAFT.

## CAM

Although, **SolidWorks** does not list all the material properties for the selected material for the cam, the maximum stress in the cam (based on its geometry distributing stresses) is approximately 71.2 MPa and can be seen in [Fig. 4-9](#). This appears to occur in tension, so if the yield strength were assumed to be close to that for AISI 316, then the yield strength could be as 172.4 MPa (as listed in **SolidWorks**) or 207 MPa (as listed in McMaster-Carr [\[3\]](#)). This would result in a factor of safety in the range of [2, 2].

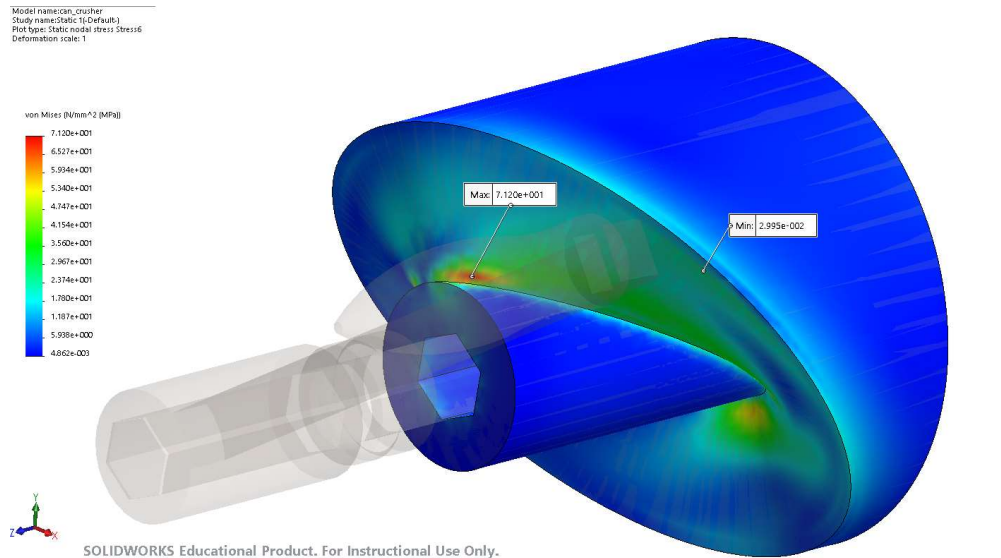


**FIGURE 4-9.** MAXIMUM STRESS OF 71.2 MPa IN THE GEOMETRY OF THE CAM.

## CHAMBER

The maximum stress in the chamber of 1412 MPa yields a factor of safety in the range of [122.10m, 146.60m]. The location of this stress is depicted in [Fig. 4-10](#).

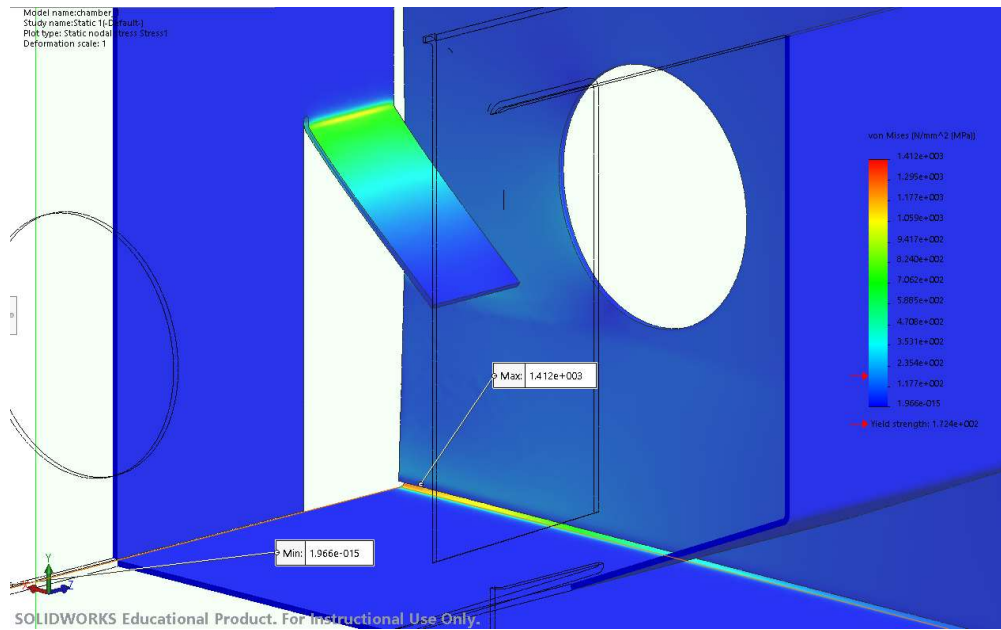


**FIGURE 4-10.** THE GREATEST STRESS SEEN IN THE CHAMBER HOUSING WAS  $1412000.0 \text{ MPa}$  AND OCCURRED AT THE FLANGE THAT MUST REACT TO THE CAN BEING CRUSHED BY THE ROTATING CAM.

#### 4.2.3. FATIGUE

This design was proposed to allow for continuous crushing of aluminum cans whether by human effort or electro-mechanically actuating the cam. Normally, such designs, which are expected to withstand many cycles during a hopefully long service life, would require a fatigue analysis. As the authors were pressed for time to complete a fatigue simulation in some FEA software, literature values seem to indicate that fatigue may be a non-issue for the proposed design.

Of the metals used throughout this analysis, the fatigue strengths of A2 tool steel ([Fig. 4-11](#)), a cast stainless steel ([Fig. 4-12](#)), AISI 316 ([Fig. 4-13](#)), and 1023 carbon steel were found to be  $\sim 265 \text{ MPa}$ ,  $\sim 400 \text{ MPa}$ ,  $\sim 250 \text{ MPa}$ , and  $\sim 225 \text{ MPa}$ , respectively [[7](#), [8](#), [9](#), [10](#)]. The stresses seen in components of these metals do not come close to some of these fatigue strengths:  $\sim 15.81 \text{ MPa}$  for the A2 tool steel inner ring of the bearings; and,  $9.171 \text{ MPa}$  shear at the AISI 316 shaft and  $34 \text{ MPa}$  in the 1023 carbon steel handle. The exception to this observation is for those stresses seen in the chamber: the  $1412000.0 \text{ MPa}$  from FEA is much greater than  $\sim 250 \text{ MPa}$  if assumed to be of similar grade steel as AISI 316.

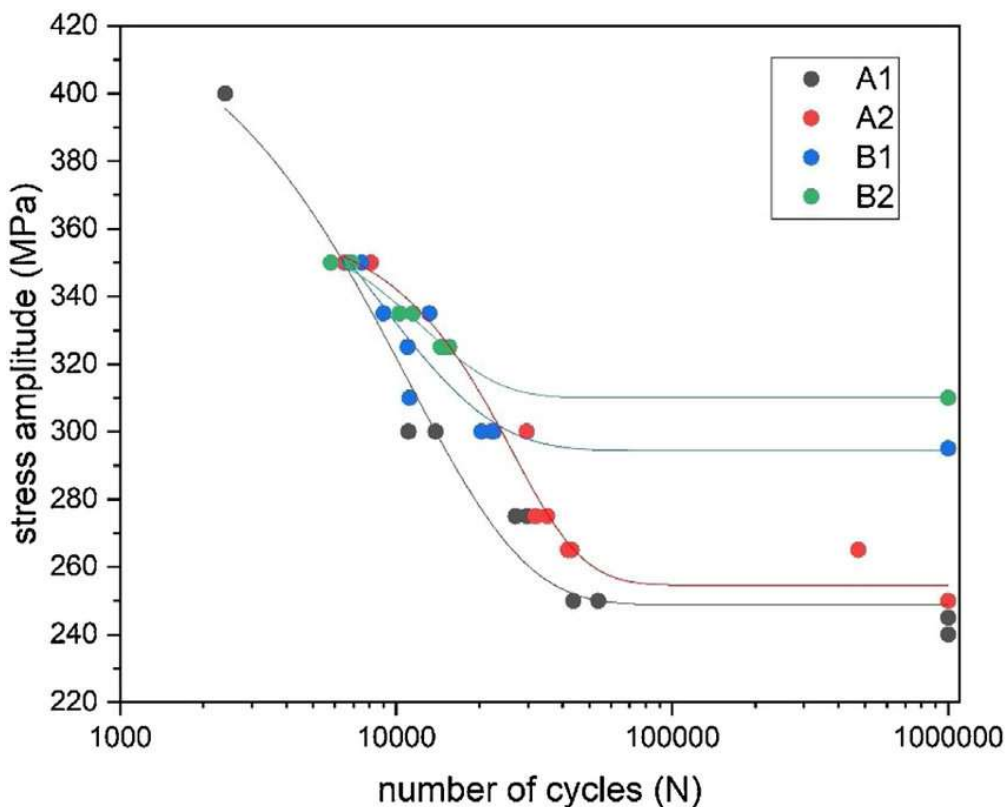


**FIGURE 4-11.** FATIGUE STRENGTH OF A2 TOOL STEEL = $\sim$  265 MPa. ADAPTED FROM [7].

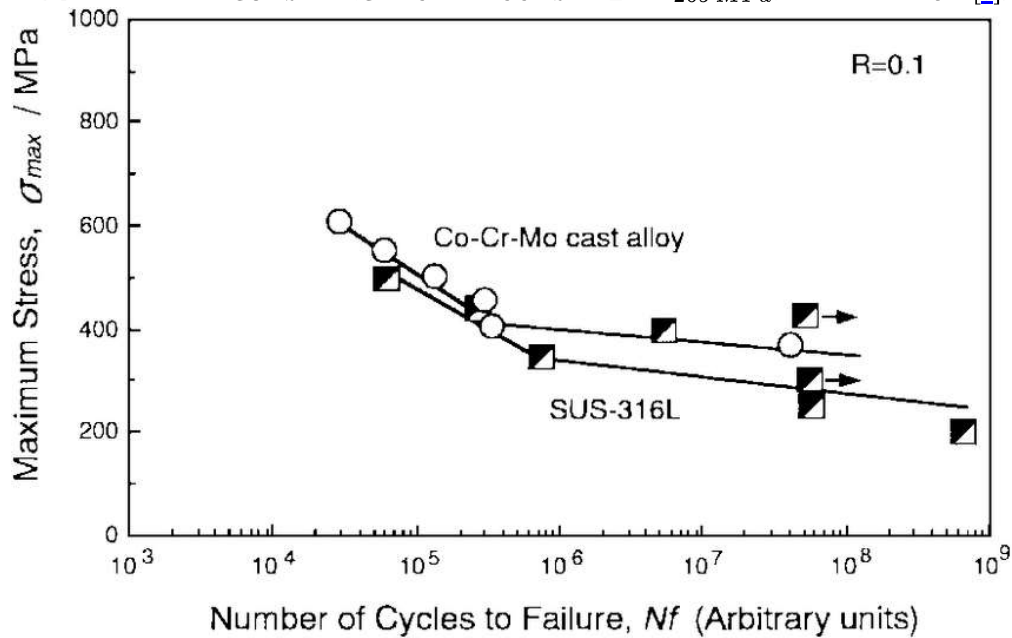


**FIGURE 4-12.** FATIGUE STRENGTH OF ONE CAST STAINLESS STEEL (CoCrMo) = $\sim$  400 MPa. ADAPTED FROM [8].

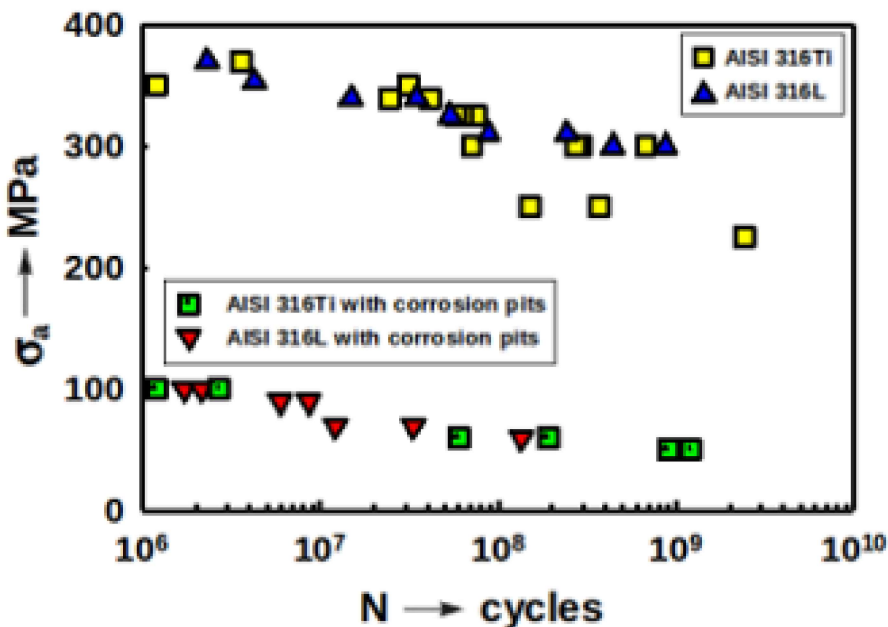


**Fig. 4.** The S-N curves of AISI 316L and AISI 316Ti steels

FIGURE 4-13. FATIGUE STRENGTH OF AISI 316 STEEL = $\sim$  250 MPa. ADAPTED FROM [9].

## 5. CONCLUSIONS

The gargantuan stress seen in the chamber (1412000.0 MPa) indicates that further work is needed in the design of the chamber housing to properly handle stress incurred from nominal operation.

## REFERENCES

- [1] Environmental Protection Agency.
- [2] J. M. Christensen, J. W. McBarron, J. T. McConville, W. R. Pogue, R. C. Williges, and W. E. Woodson, "Man-Systems Integration Standards NASA-STD-3000, Volume II Revision B, July 1995."
- [3] McMaster-Carr, "Corrosion-Resistant 316/316L Stainless Steel Hex Bar 1' Wide." 2021.
- [4] McMaster-Carr, "Crank Handle with Machinable Solid Hub, 11' Center-to-End Width." 2021.
- [5] A. Ugural and S. Fenster, *Advanced Mechanics of Materials and Applied Elasticity (International Series in the Physical and Chemical Engineering Sciences)*, Sixth. Pearson, 2019.
- [6] "Overview of Materials for Stainless Steel." [https://www.matweb.com/search/datasheet\\_print.aspx?matguid=71396e57ff5940b791ece120e4d563e0](https://www.matweb.com/search/datasheet_print.aspx?matguid=71396e57ff5940b791ece120e4d563e0).
- [7] P. Jovičević-Klug and B. Podgornik, "Comparative Study of Conventional and Deep Cryogenic Treatment of AISI M3:2 (EN 1.3395) High-Speed Steel," *Journal of Materials Research and Technology*, vol. 9, pp. 13118–13127, Sep. 2020, doi: 10.1016/j.jmrt.2020.09.071.
- [8] Y. Okazaki and E. Gotoh, "Corrosion Fatigue Properties of Metallic Biomaterials in Eagle's Medium," *Materials Transactions - MATER TRANS*, vol. 43, pp. 2949–2955, Dec. 2002, doi: 10.2320/matertrans.43.2949.
- [9] F. Nový, V. Zatkálíková, O. Bokůvka, and K. Miková, "Gigacycle Fatigue Endurance of Marine Grade Stainless Steels with Corrosion Pits," *Per. Pol. Transp. Eng.*, vol. 41, no. 2, p. 99, 2013, doi: 10.3311/PPtr.7109.
- [10] "SAE-AISI 1023 (G10230) Carbon Steel MakeItFrom.Com." <https://www.makeitfrom.com/material-properties/SAE-AISI-1023-G10230-Carbon-Steel>.



